Smoothening mechanism for GaAs(100) surfaces during ion-enhanced plasma etching

S. H. Lee and H. P. Gillis[a]
Department of Materials Science and Engineering, University of California, Los Angeles, California 90095

C. Ratsch
Department of Mathematics, University of California, Los Angeles, California 90095

(Received 15 November 2005; accepted 7 March 2006; published online 20 April 2006)

We present experimental data showing the development of smooth surfaces on GaAs(100) exposed simultaneously to ion bombardment and reactive species in chlorine plasma. With negligible ion bombardment, the surface develops ⟨110⟩ ridges and {111} facets, as in purely chemical etching. With ion bombardment at energy 27 eV, formation of ridges and facets is reduced, and at 110 eV the etched (100) surface has a root-mean-square roughness of 0.5 nm. Kinetic Monte Carlo simulations suggest that low energy ion bombardment modifies the relative ratios of reaction rates at specific sites from their purely chemical values to give the smooth surface. © *2006 American Institute of Physics*. [DOI: 10.1063/1.2196063]

The purpose of etching is to transfer features from a device design mask to an underlying film of device material, replicating accurately the cross-sectional profile of each feature. In addition to controlling the critical dimensions of device features, producing smooth etched surfaces is essential. There have been a few studies of the mechanisms for morphology development during wet etching,[1] etching by oxygen atoms at 5 eV,[2] and ion sputtering,[3] but none on the ion-enhanced dry etching processes used in device fabrication.

This study is concentrated on the mechanism by which extremely smooth surfaces can be obtained when etching GaAs(100) in chlorine plasma. Previous work has produced root-mean-square (rms) roughness of 0.9–1.5 nm,[4] and one recent study reported 0.6 nm.[5] We have identified conditions in inductively coupled plasma (ICP) etching that give rms roughness of 0.5 nm.[6] We have developed a simple physicochemical model to describe the transition from rough, faceted surfaces (thermochemical etching) to smooth surfaces (thermochemical etching with ion bombardment).

Samples were *n*-type GaAs(100) "epiready" wafers doped to $0.5-5\times10^{18}$ cm^{-3} with Si.[7] Experiments were conducted in a Unaxis SLR 770 ICP etching system, which provides independent control of the ion flux to the sample and ion bombardment energy at the sample. All studies used a gas mixture of boron trichloride (100 sccm [sccm denotes cubic centimeter per minute at STP]) and chlorine (60 sccm) with a steady state pressure of 18 mTorr. The sample temperature was 283 K. Each sample had an initial cleaning process (900 W plasma power, 100 W bias power, and 10 s duration) to remove native oxide. After cleaning, each sample was etched for 5 min, using bias power of 0, 12, 20, or 50 W with plasma power of 900 W.

The energy of the ions is varied systematically by changing the sample bias. Positive ions are accelerated to the sample with an average energy E_i determined by the difference between the plasma potential V_p and the negative dc offset potential V_{dc}. Table I shows the measured values of V_{dc} and the corresponding ion energies for each sample. Plasma potential was not measured; the value 25 V negative from earth, measured in identical ICP systems operating under similar conditions and gas composition, has been used here.[8] At no bias, arrival energy of the ions is controlled by the difference between plasma potential V_p and the floating potential V_f. In Table I this value is calculated from $V_p - V_f = T_e \ln(M/2\pi m)^{1/2}$, where M is the mass of the gas molecules, m is the electron mass, and T_e is the electron temperature; we used the value T_e=4 eV, typical for ICP plasmas.[9] Constancy of ion flux to the sample is confirmed by the linear increase of V_{dc} values in Table I with bias power.[10] The ion flux is proportional to the slope of this linear increase; its value is 5.6 mA cm^{-2} or 3.5×10^{16} ions cm^{-2} s^{-1}. With no bias applied, the sample is at the floating potential of the plasma, where the etching is almost purely chemical. The flux of neutral reactive species such as Cl atoms is determined by the percent dissociation, which depends on source power, reactor geometry, gas composition, and pressure, among other variables and is difficult to estimate analytically. The percent dissociation is not known in our experiments, but is held constant by keeping constant all the contributing variables. We systematically vary the energy of ion bombardment at the constant ion flux of 3.5×10^{16} ions cm^{-2} s^{-1} and constant but unknown flux of reactive species. If we assume a conservative 50% dissociation,[11] the flux of Cl atoms to the surface will be 2.9×10^{17} at. cm^{-2} s^{-1}, ten times larger than the measured ion flux. In beam experiments where the ion/neutral flux ratio is controlled directly, the saturation region corresponds to our plasma conditions.[12] More details will be given elsewhere.[13]

Figure 1 shows etch depth, scanning electron microscopy (SEM) images, atomic force microscopy (AFM) line scans, and rms roughness for a sample run at each set of conditions. (Before etching, each of these samples had rms roughness of 0.2–0.3 nm.) The surface morphology is dominated by ridges that become smaller in height and closer together as ion energy increases, disappearing to give a very

TABLE I. Bias power, bias voltage, and ion energy applied to samples.

Bias power (W)	0	12	20	50
Bias voltage (V)		−52	−70	−135
Ion energy (eV)	20	27	45	110

[a]Author to whom correspondence should be addressed; electronic mail: hpgillis@ucla.edu

 © 2006 American Institute of Physics
Downloaded 05 Sep 2006 to 128.97.46.57. Redistribution subject to AIP license or copyright, see http://apl.aip.org/apl/copyright.jsp

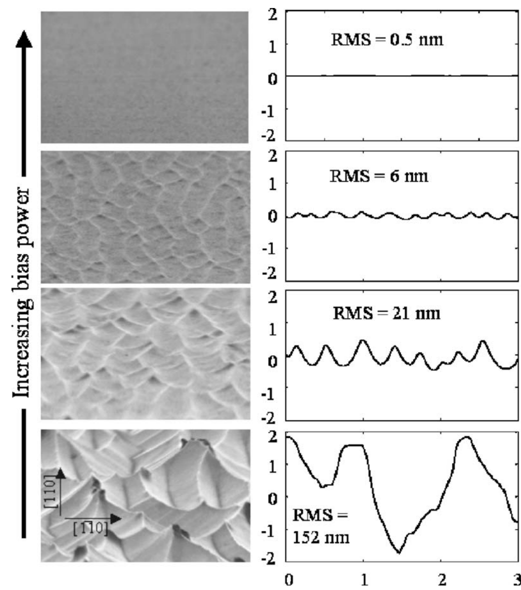

FIG. 1. Scanning electron microscopy (SEM) images (left column), atomic force microscopy (AFM) line scans (right column), and root-mean-square (rms) roughness (inset in AFM profiles) of a sample run at each set of conditions. All SEM and AFM images span 3 μm horizontally. The scale on the line scans is 100 nm for the vertical axis and 1 μm for the horizontal axis. Bias power values (and etch depths) are 0 W (24.4 μm), 12 W (23.5 μm), 20 W (24.4 μm), and 50 W (24.5 μm). Source power was held at 900 W for 5 min etching.

Configuration	NN	NNN	Rate constant
(1)	0	0	k_{column}
(2)	0	1	$k_{vertical}$
(3)	0	2	k_{ridge}
(4)	1	1	$k_{vertical}$
(5)	1	2	$k_{vertical}$
(6)	1	2	k_{step}
(7)	1	3	$k_{\{111\}}$
(8)	2	2	$k_{\{100\}}$
(9)	2	3	$k_{\{111\}}$
(10)	2	4	$k_{\{111\}}$

FIG. 2. Definitions of site-specific etch rates. The shaded square represents the site, in the first or second layer of the solid, whose etch rate is being defined. The first row of three squares below the active site represents the first bulk layer of the solid. Site-specific rates are determined by the number of nearest neighbors (NNs) and next nearest neighbors (NNNs), and the stability of facets, in particular, for the (111) (configuration 7) and (100) (configuration 8), as stated in the text.

smooth surface at 110 eV. In each, the (100) surface of the sample is in the plane of the image. The sample at no bias shows ridges in the [110] direction, from which the etched surface slopes down at ca. 55°. The sloped faces are therefore the $\{111\}A$ Ga-filled planes. Other ridges intersect the first group at 45°; from these, surfaces sloping down at ca. 55° are the $\{111\}B$ As-filled planes. This topography has been seen on GaAs(100) in a variety of wet,[14] high-temperature,[15] and plasma[16] etch recipes. Figure 1 demonstrates that at no bias power the etching is primarily chemical, with results similar to "hillock formation" in the wet etching of silicon.[17] The challenge is to explain how ion bombardment causes the transition from chemical etching to produce a smooth surface.

We have developed a simple cubic two-dimensional Kinetic Monte Carlo (KMC) model, where one dimension is the lateral dimension and the other one is the height, to initially explore the relation between site-specific chemical etch rates and ion bombardment. KMC simulations have previously been used to model shallow etch pits in a simple cubic model and on diamond {111} surfaces. KMC simulations specific to wet etching of Si(111) have shown that surface morphology is controlled by the relative rates of reactions at different specific sites.[18] In our simulations, atoms are removed at a site-specific etch rate k_i, determined not by counting bonds, but rather by considering the different possible facets (cf. Fig. 2). We assume that k_i is typically higher at sites with high-index planes. We define *a priori* relative values for those k_i justified by published rate data, and then vary systematically the other k_i. References 14–16 establish the relative order on different planes of GaAs under chemical conditions as $k_{\{111\}A} < k_{\{100\}} < k_{\{111\}B} < k_{(\text{higher order planes})}$; specifically, $k_{\{111\}A}:k_{\{100\}}=1:5-8$, and we use the ratio 1:7.[19] It is intuitively clear that an atom with no nearest neighbor (NN) or next nearest neighbor (NNN) is bound less strongly (configuration 1 in Fig. 2), so we set $k_{column}:k_{\{111\}}=1000:1$. On the other hand, it is plausible that sites with 2 NN and 3 or 4 NNN (configuration 9 and 10) should be rather stable, so we set their rates equal to $k_{\{111\}}$. Sites with 0 NN and 1 NNN (configuration 2) and with 1 NN and 1 or 2 NNN (configurations 4 and 5) are very similar in that one side (in the figure, left), which is columnlike, while the other is a low index plane [either (100) or (111)]. We therefore assign the same $k_{vertical}$ to all of these configurations. The morphology is then determined by competition between $k_{vertical}$ and the remaining k_{step} (configuration 6) and k_{ridge} (configuration 3).

We have systematically varied $k_{vertical}$, k_{step}, and k_{ridge} from 1 to 1000. We have tracked the surface morphology and calculated rms roughness on a lattice of size 5000 through removal of 1000 layers. We tested that the results are independent of the system size, and are essentially the same for different etch depths. We find that the dependence is strongest on k_{ridge}, and that the effects of $k_{vertical}$ and k_{step} are similar; hence, in Fig. 3 we show a two-dimensional contour plot of surface roughness obtained with $k_{vertical}=k_{step}$. We always start with a perfect (100) surface, from which atoms are removed to create "pit sites" (configuration 10). At some of these the resulting steps flow in either direction with rate k_{step}; at others the "pit atom" is removed with rate k_{111} to create double steps on either side. These "double steps" become short (111) facets by losing a single atom, in competition with flow of single steps. These interactions of pits and steps can move in both directions to create "ridge" sites (configuration 3) in which a single atom is exposed. As long as k_{ridge} remains small, and k_{step} is large enough, etching is dominated by interaction of pits and steps in the regions between the (slowly etching) ridges. The result is a rough surface, with morphology dominated by the heights of the ridges and distances between them. This can be seen in Fig. 3, where the highest rms values are in the lower right corner.

Downloaded 05 Sep 2006 to 128.97.46.57. Redistribution subject to AIP license or copyright, see http://apl.aip.org/apl/copyright.jsp

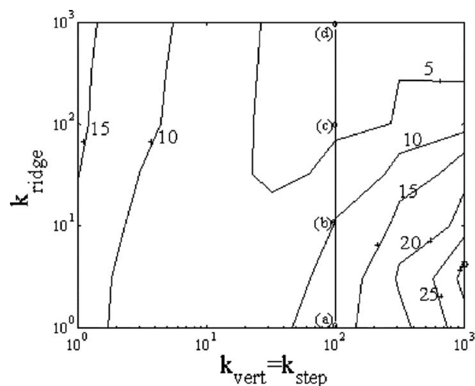

FIG. 3. Contour plot of rms roughness as a function of etch rates k_{ridge}, k_{vertical}, and k_{step} after 1000 layer etching with $k_{\mathrm{column}}=1000$, $k_{\{111\}}=1$, and $k_{\{100\}}=7$.

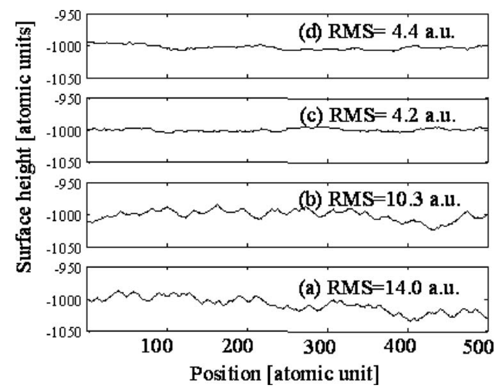

FIG. 4. Surface profiles along the dotted line in the rms contour plot in Fig. 3. Etch rates k_{vertical} and k_{step} are held at 100, and k_{ridge} is varied as (a) 1, (b) 10, (c) 100, and (d) 1000.

As k_{ridge} increases, etching is dominated by step flow, and the surface is much smoother.

In Fig. 4 we show typical morphologies at an etch depth of 1000 layers for $k_{\mathrm{vertical}}=k_{\mathrm{step}}=100$, with k_{ridge} varying from 1 to 1000. Clearly, the surface is very smooth for $k_{\mathrm{ridge}}=1000$, and becomes rougher with saw-tooth-like features as k_{ridge} decreases. The development of the (111) facets with decreasing k_{ridge} and the resulting increase in rms roughness are shown in Fig. 4. When k_{ridge} is small, more than 60% of the sites are of type (111). As can be seen in Fig. 4, this does not imply a monolithic (111) face. About 8% of the sites are ridges, and the (111) sites must appear on the down-sloping sides of the ridges. When k_{ridge} is large, the number of ridges goes essentially to zero, the number of (111) sites is dramatically reduced, and the (smooth) surface is dominated by (100) sites. More than 50% of sites are of type (100) (configuration 8 in Fig. 2).

The results of the simulation rationalize the trend in experimental results in Fig. 1. Although ions are not explicitly included in the simulation, it is intuitively clear that ions with sufficient energy will effectively increase the reaction rate at all sites, shifting the relative values of site-specific reaction rates away from their purely chemical values. Our simulations then suggest that this increase is more relevant at sites that are more exposed to ion bombardment than others, increasing k_{ridge} preferentially over other rates. This conclusion is physically plausible, even in the absence of a detailed scattering model of ion bombardment at the different types of sites. Among the three competing configurations 3, 4, and 6, only the ridge atom in 3 is exposed on all sides, and can be easily dislodged by low energy ions, effectively increasing k_{ridge} more than the other rates. Similarly, ions with energies well below sputtering thresholds can induce surface atom displacement and migration effects that influence surface morphology in film growth.[20] In Fig. 1, enhancement of k_{ridge} is already under way at 27 eV. As the ion energy increases, these low energy surface atom displacements will continue to occur and enable smooth surfaces, while now the ions can also penetrate beneath the surface and generate the linear collision cascades that dominate the rate of ion-enhanced etching.[21] This smoothening mechanism is valid when the flux of reactive neutral species is large compared to the flux of ions.

Previous mechanistic studies in ion-enhanced etching have been concerned primarily, showing that the ion bombardment enables the "straight sidewalls," which are required to control critical dimensions of microdevices,[22] and that the enhancement is driven by linear collision cascades. This work has identified a different mechanism at lower ion energy, through which ion bombardment modifies surface morphology by shifting relative values of site-specific reaction rates through displacements of more weakly bound surface atoms.

The authors are grateful for discussions with Professor Jane P. Chang, Professor Mark S. Goorsky, and Professor Ya-Hong Xie.

[1]M. E. R. Dotto and M. U. Kleinke, Physica A **295**, 149 (2001); M. Saitou, M. Hokama, and W. Oshikawa, Appl. Surf. Sci. **185**, 79 (2001).
[2]T. Ngo, E. J. Snyder, W. M. Tong, R. S. Williams, and M. S. Anderson, Surf. Sci. **314**, L817 (1994).
[3]E. A. Eklund, R. Bruinsma, J. Rudnick, and R. S. Williams, Phys. Rev. Lett. **67**, 1759 (1991); Z. Moktadir, K. Sato, A. Mastumuro, K. Kayukawa, and M. Shikida, Mater. Res. Soc. Symp. Proc. **605**, 305 (2000).
[4]K. D. Choquette, R. J. Shul, A. J. Howard, D. J. Rieger, R. S. Freund, and R. C. Wetzel, J. Vac. Sci. Technol. B **13**, 40 (1995); A. R. Giehl, M. Gumbel, M. Kessler, N. Herhammer, G. Hoffmann, and H. Fouckhardt, J. Vac. Sci. Technol. B **21**, 2393 (2003).
[5]W. T. Lim, I. G. Baek, P. G. Jung, J. W. Lee, G. S. Cho, J. I. Lee, K. S. Cho, and S. J. Pearton, J. Electrochem. Soc. **151**, G163 (2004).
[6]These conditions also give straight sidewalls on masked samples, but that result is not the focus of this study.
[7]Purchased from Wafer Technology Ltd., Milton Keynes, Bucks, UK.
[8]D. C. Hays, M.S. thesis, University of Florida, 1999.
[9]M. A. Lieberman and A. J. Lichtenberg, *Principles of Plasma Discharges and Materials Processing* (Wiley, New York, 1994).
[10]I. I. Amirov, M. O. Izyumov, and O. V. Morozov, High Energy Chem. **37**, 328 (2003) [K'o Hsueh Yueh K'an **37**, 373 (2003)].
[11]M. V. Malyshev, V. M. Donnelly, A. Kornblit, and N. A. Ciampa, J. Appl. Phys. **84**, 137 (1998).
[12]J. P. Chang, A. P. Mahorowala, and H. H. Sawin, J. Vac. Sci. Technol. A **16**, 217 (1998).
[13]S. H. Lee, H. P. Gillis, and C. Ratsch (unpublished).
[14]D. W. Shaw, J. Cryst. Growth **47**, 509 (1979); D. W. Shaw, J. Electrochem. Soc. **128**, 874 (1981).
[15]M. Heyen and P. Balk, J. Cryst. Growth **53**, 558 (1981).
[16]D. E. Ibbotson, D. L. Flamm, and V. M. Donnelly, J. Appl. Phys. **54**, 5974 (1983); H. P. Gillis, D. A. Choutov, K. P. Martin, and Li Song, Appl. Phys. Lett. **68**, 2255 (1996).
[17]J. Flidr, Y.-C. Huang, and M. A. Hines, J. Chem. Phys. **111**, 6970 (1999).
[18]M. A. Hines, Annu. Rev. Phys. Chem. **54**, 29 (2003).
[19]Our model cannot distinguish the {111}*A* and {111}*B* planes. Henceforth, {111} refers to the {111}*A* planes that dominate the chemical etching morphology. Only the relative values of the site-specific rates are important; we set $k_{\{111\}}=1$ and state values of other k_i relative to it.
[20]C.-H. Choi, R. Ai, and S. A. Barnett, Phys. Rev. Lett. **67**, 2826 (1991).
[21]C. Steinbrüchel, Appl. Phys. Lett. **55**, 1960 (1989).
[22]J. W. Coburn and H. F. Winters, J. Appl. Phys. **50**, 3189 (1979); H. F. Winters and J. W. Coburn, Surf. Sci. Rep. **14**, 161 (1992).

Downloaded 05 Sep 2006 to 128.97.46.57. Redistribution subject to AIP license or copyright, see http://apl.aip.org/apl/copyright.jsp